Preparation and Characterization of SO_4^{2-}/TiO_2-HBeta for Selective Conversion of 1-Methylnaphthalene

Hao SUN [1, 2], Xin HUANG [1], Junjian ZHU [1], Zhenggui GU [1, 2] *

[1] *College of Chemistry and Materials Science, Nanjing Normal University, Nanjing 210023, P. R. China*
[2] *Jiangsu Provincial Key Laboratory of Materials Cycling and Pollution Control, Nanjing Normal University, Nanjing 210023, P. R. China*

crossref http://dx.doi.org/10.5755/j01.ms.23.2.16679

Received 05 November 2016; accepted 25 December 2016

In this study, new types of SO_4^{2-}/TiO_2-HBeta (ST/Hβ) catalysts are synthesized and characterized by XRD, IR, N_2 adsorption-desorption, ICP-OES, SEM, and NH_3-TPD methods. Conversion of 1-methylnaphthalene is carried out in a fixed-bed system. Based on the study's results, the catalysts ST/Hβ showed uniform SO_4^{2-}/TiO_2 (ST) loading, high surface area, and sufficient mild acid sites. When ST content increased, the amount of strong acid sites and by-products decreased. Under atmospheric pressure, catalyst 15-ST/Hβ showed a catalytic performance of 74.1 % conversion and 97.4 % selectivity.

Keywords: sulfated titanium oxide, Beta zeolite, characterization, 1-methylnaphthalene, catalytic properties.

1. INTRODUCTION

Polyethylene naphthalate (PEN) is an advanced polymer material with favorable electrical, mechanical, and thermal properties [1]. In recent decades, the synthesis of 2,6-dimethylnaphthalene (2,6-DMN) from naphthalene (NA) and 2-methylnaphthalene (2-MN) has received much attention [2 – 4] as the key precursor of PEN. The selective isomerization of dimethyl naphthalene (DMN) mixtures to 2,6-DMN [5 – 7] has also been explored. The explosive utilization of the PEN precursor has motivated research on the selective conversion of 1-methylnaphthalene (1-MN) to NA, 2-MN, and DMN.

In prior studies [8 – 11] and our recent study [12], Beta (β) zeolite has been demonstrated as an effective catalyst for the conversion of 1-MN due to its thermal stability and appropriate pore size distribution in comparison with other zeolites. However, by-products during the synthesis process are unavoidable, given the excessive strong acidic sites of H-Beta (Hβ) [3, 13, 14]. To overcome this disadvantage, several methods were developed based on the modification of the zeolite's acidic sites, such as silylation [4], ion exchange [15], and dealumination [16]. A limited number of studies have reported the coupling of other acidic sites.

SO_4^{2-}/M_xO_y solid acid catalysts possess a new kind of acidic sites, and they have recently attracted attention due to their easy separation, reduced environmental impact, and low by-product generation [17, 18]. Sulfated titanium oxide (ST) and sulfated zirconia (SZ) are of particular interest [19 – 21]. Additionally, SZ and ST were also shown to be modifiable on mesoporous materials, enabling the materials to generate controllable acidic properties [22 – 24]. Further, owing to ST solid acids' adjustable acidity, the strength of acid sites varies with different preparation conditions [25, 26]. Therefore, we envision that the Hβ zeolites with ST modification could improve the selectivity of alkyl naphthalene (AN). The goal is to dispersedly support moderate ST on microporous Hβ for this outstanding property.

Prasetyoko et al. [27] have reported the synthesis of microporous zeolite loaded with SZ. In our recent unpublished work, zeolite Hβ loaded with ST and synthesized by the above method showed much lower BET surface area, catalytic conversion, and stability. This might be attributed to pore blocking during the synthesis process [28]. In the current work, we synthesized a new type of ST/Hβ catalyst by supporting ST on template containing zeolite Hβ with one-step synthesis. We investigated in detail the effects of ST content on texture, acidity, and catalytic performance of catalyst ST/Hβ.

2. EXPERIMENTAL DETAILS

2.1. Materials

1-methylnaphthalene (≥ 98 %) was purchased from Aladdin Reagent Co., Ltd., China. Titanium sulfate [$Ti(SO_4)_2$] was purchased from Sinopharm Chemical Reagent Co., Ltd., China. Template containing zeolite NH_4Beta (Si/Al = 24) was synthesized according to Ref. [29].

2.2. Catalyst preparation

ST-loaded Beta was obtained by the wet impregnation method. We mixed 2 g NH_4Beta with $Ti(SO_4)_2$ in water. The suspension was stirred and dried. The treated sample that calcined at 550 °C (heating rate: 2 °C/min) in air was referred to as X-ST/Hβ, based on the titanium content in the catalyst. Sulfated titanium oxide (ST) was synthesized by grinding $Ti(SO_4)_2$ in a mortar. After that, the sample was dried and calcined at 550 °C (heating rate: 2 °C/min) for 5 h in air. Table 1 summarizes the percentage of titanium in the samples and their treatments.

* Corresponding author. Tel.: +86-25-83598233; fax: +86-25-83598233.
E-mail address: *guzhenggui@njnu.edu.cn* (Z.G. Gu)

2.3. Characterization

Table 1. Titanium content of the samples[a]

Sample	Ti content, *wt.*%
Hβ	0[b]
10-ST/Hβ	10.3[c]
15-ST/Hβ	15.2[c]
20-ST/Hβ	20.5[c]

[a] Calculated by ICP-OES;
[b] The sample was prepared by calcining NH_4Beta at 550 °C for 5 h;
[c] After the impregnation of 0.2, 0.3, and 0.4 mol/L $Ti(SO_4)_2$ respectively, the sample was dried and calcined at 550 °C for 7 h.

Inductively coupled plasma optical emission spectrometer (ICP-OES) was acquired on a Thermo IRIS Intrepid II instrument. X-ray diffraction (XRD) analysis was conducted with a Rigaku D/max-2500 using Cu Kα radiation and operating at 100 mA and 40 kV. Fourier transform infrared (FTIR) spectroscopy was conducted on a Nicolet 520 SXFTIR spectrometer in the mid IR region (400-4000 cm^{-1}). The N_2 sorption was carried out on a Micromeritics ASAP 2460 volumetric adsorption apparatus at – 196 °C using liquid N_2. We observed the surface morphology on a Hitachi S-4800 scanning electron microscope (SEM), coupled with energy dispersive X-ray spectroscopy (EDS). NH_3 temperature-programmed desorption (NH_3-TPD) was studied on a TP-5000 instrument coupled with a thermal conductivity detector. Thermogravimetric analysis (TG) was determined with a PerkinElmer Diamond TG/DTA instrument in O_2 atmosphere.

2.4. Catalytic reaction

The conversion of 1-MN was conducted in a continuous flow fixed-bed system (Fig. 1) containing 12 g of catalyst at 380 °C under atmospheric pressure. The 1-MN was fed into the preheating section with a flow rate of 0.1 ml/min. Products were obtained at regular intervals and analyzed via gas chromatography (ThermoFisher Trace 1300) equipped with a capillary column (SE-30). We used a GC–MS (Varian 3800/2200) equipped with Varian cp-sil-19 column for product identification. Catalysts' catalytic activity was obtained by calculating 1-MN conversion and AN selectivity.

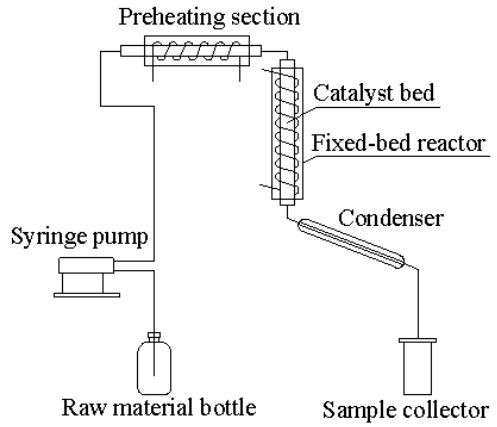

Fig. 1. Conversion of 1-MN in fixed-bed system

3. RESULTS AND DISCUSSION

3.1. Catalyst characterization

Fig. 2 shows the crystal structure measured by XRD. The bare ST sample exhibits diffraction peaks ascribed to rutile- and anatase-phase crystal planes [30]. In the case of the X-ST/Hβ catalysts, the Beta framework (*BEA) structure is retained, whereas the crystallinity of Hβ decreases when ST content increases. This can be attributed to the decrease in the samples' Beta percentage. Taking the 20-ST/Hβ catalysts as an example, TiO_2 with anatase phase exhibits a clear diffraction peak at 25.3°.

Fig. 3 a plots the IR spectra for ST. There are four obvious bands at 991, 1046, 1134, and 1225 cm^{-1} associated with chelating bidentate sulfate ion coordinated to titanium cations [31]. At 1633 and 3404 cm^{-1}, two bands assigned to the vibrations of OH groups feature titanium oxide [30]. Therefore, simply with drying and calcination of $Ti(SO_4)_2$, ST can be synthesized successfully.

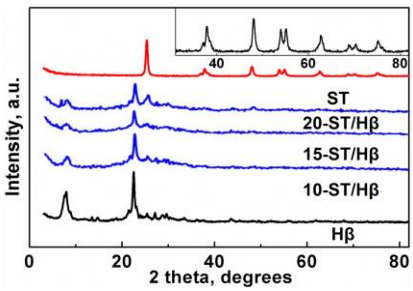

Fig. 2. XRD profiles of catalysts and partial magnification (inset) of ST

Fig. 3 b depicts the IR spectra of zeolite lattice vibration. All samples show obvious bands at 518, 527, and 539 cm^{-1} ascribed to the internal linkages in AlO_4 (or SiO_4) tetrahedral, since their intensities are closely related to tetragonal and monoclinic systems [32, 33]. We can also see that the intensity of the 991 cm^{-1} band, which is symmetric stretching of the S–O vibrations, evidently increases after ST loading. Accordingly, the *BEA structure is maintained and a special ST structure is supported on the modified Hβ's surface. This is further confirmed by the XRD results.

The isotherms measured for the zeolite Beta can be identified as type I, typical of purely microporous material (Fig. 4). Correspondingly, HK pore size distribution is at a median value of 0.55 nm (inset). Table 2 lists the S_{BET}, median pore width, and pore volume of ST, Hβ, and X-ST/Hβ catalysts.

Table 2. Textural properties of ST, Hβ and X-ST/Hβ

Sample	S_{BET}, m^2/g	Pore volume, cm^3/g	Micropore area, m^2/g	HK median pore width, nm
Hβ	371	0.427	220	0.55
ST	114	0.461	-	-
10-ST/Hβ	326	0.345	204	0.56
15-ST/Hβ	315	0.338	189	0.56
20-ST/Hβ	254	0.296	172	0.54

We find that the ST sample with simple calcination shows a S_{BET} of 114 m^2/g.

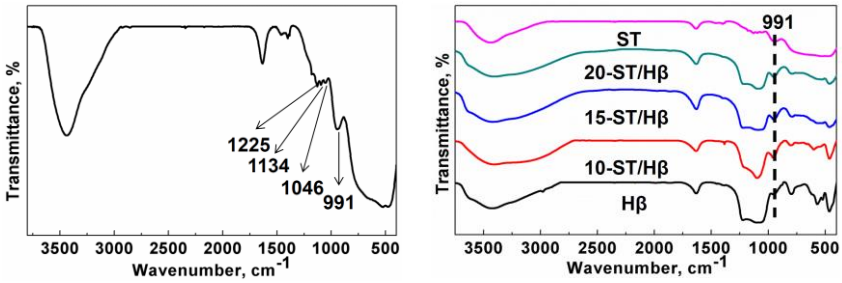

Fig. 3. IR spectra of catalysts: a – ST; b – Hβ and X-ST/Hβ

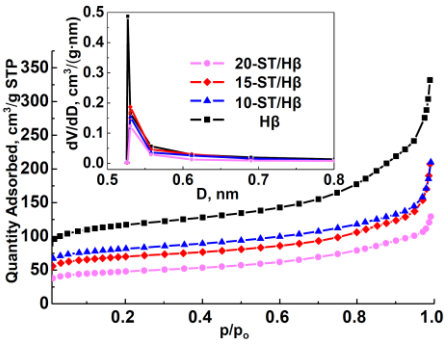

Fig. 4. Adsorption isotherms of N_2 and HK pore size distribution (inset) of the Hβ and X-ST/Hβ

For samples of 10-15-ST/Hβ, the specific surface area is much higher (315 – 326 m^2/g) than that of ST. Further, the HK pore size distribution of X-ST/Hβ shows a mean value of approximately 0.54 – 0.56 nm, indicating the same internal microporous structure as Hβ.

Fig. 5 and Fig. 6 show, respectively, SEM images and EDS of catalyst 10-ST/Hβ. The catalyst 10-ST/Hβ exhibits uniform particles with 30 nm diameter. As demonstrated by EDS mapping, homogeneous distribution and density of different elements are evident on the entire surface of 10-ST/Hβ [34]. This is consistent with XRD, IR and, BET analyses, indicating that ST species on the surface of Hβ are highly dispersed.

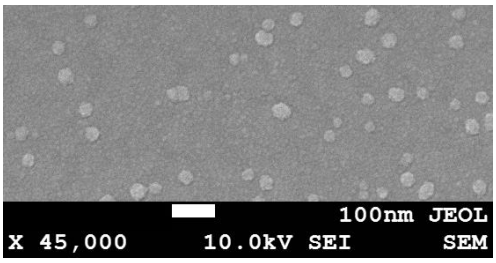

Fig. 5. High magnification SEM of 10-ST/Hβ

The amount and strength of acid sites on the catalyst surface were determined by NH_3-TPD. As Fig. 7 shows, three major NH_3 desorption peaks appear in the ranges of 150-350 °C (weakly acidic sites), 350-500 °C (moderately-strong acidic sites), and 500-700 °C (strong acidic sites), respectively [35]. With simply calcination of $Ti(SO_4)_2$, only weak and medium acidic sites are observed on the surface of ST.

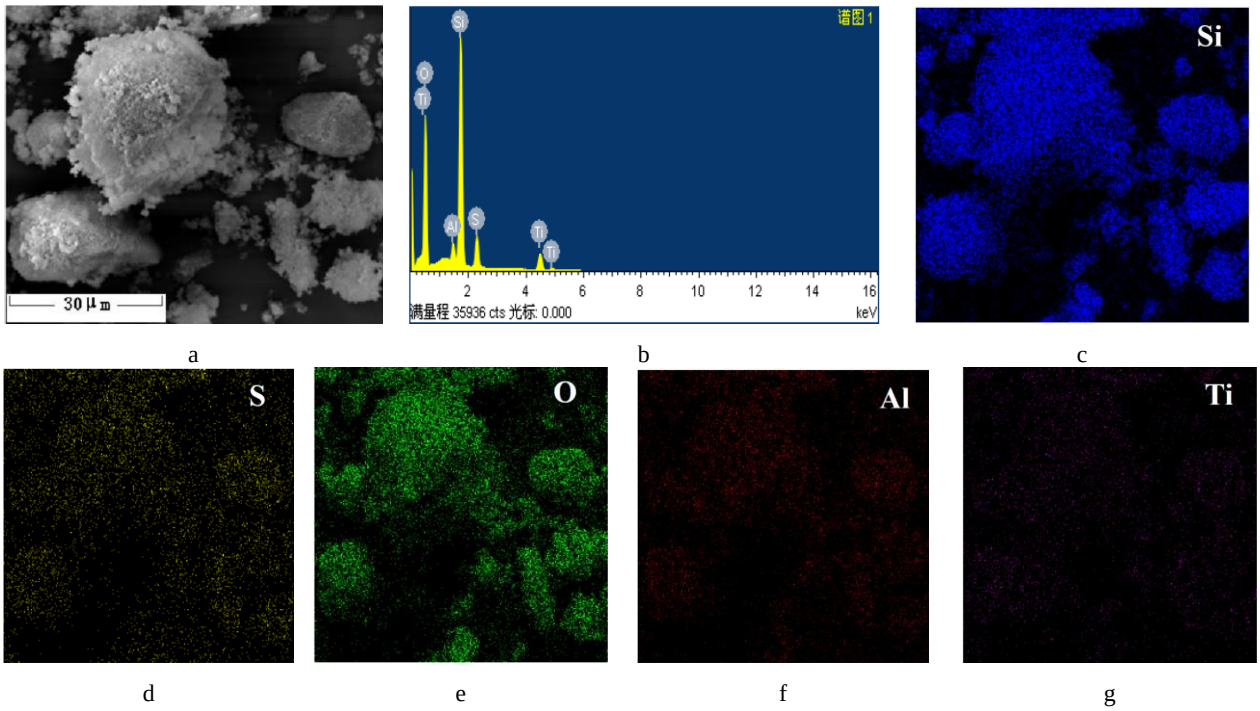

Fig. 6. The SEM and EDS of 10-ST/Hβ: a – SEM; b – Mass ratios of elements; c – EDS map of Si; d – EDS map of S; e – EDS map of O; f – EDS map of Al; g – EDS map of Ti

For the samples of X-ST/Hβ, it is clear that the strong acid sites markedly diminish after ST is loaded on Hβ, whereas the weak and moderately strong acidic sites remain stable.

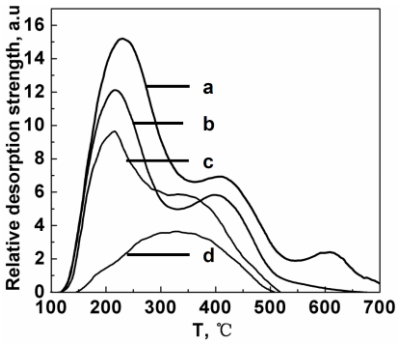

Fig. 7. NH_3-TPD curves: a – Hβ; b – 15-ST/Hβ; c – 20-ST/Hβ; d – ST

3.2. Catalyst activity

Table 3 lists the product distribution and catalytic activity of Hβ, ST, and X-ST/Hβ. As Scheme 1 shows, the main products of 1-MN conversion are 2-MN, NA, and DMN. With ST content increasing from 10 to 20 % (by mass), the AN selectivity over X-ST/Hβ is enhanced from 95.08 % to 99.37 %, which is higher than Hβ. Based on the NH_3-TPD results, we might conclude that the strong acid sites are responsible for side reactions, such as dealkylation and cracking [3]. Substantial weak and moderately strong acidic sites are favourable for the high catalytic conversion. Meanwhile, due to the internal microporous structure [13], catalysts 15-20-ST/Hβ exhibit higher AN selectivity than ST. As Fig. 8 depicts, 15-20-ST/Hβ presents relatively stable AN selectivity with TOS.

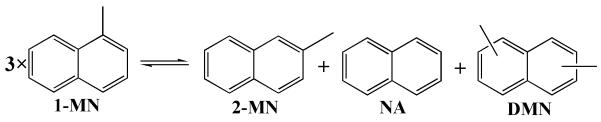

Scheme 1. Main reactions for the conversion of 1-MN

Table 3. Reaction data of ST, Hβ, and X-ST/Hβ for conversion of 1-MN[a]

Distribution, %	Hβ	ST	X-ST/Hβ		
			10	15	20
Light fraction (C_6-C_9)	4.43	0	2.55	1.93	0.20
Heavy fraction (>C_{12})	1.02	0.90	1.09	0.22	0.22
1-MN	26.44	76.44	25.97	25.89	32.75
NA	4.57	7.35	6.83	9.13	9.87
2-MN	57.43	14.62	56.28	54.31	52.32
DMN	6.11	1.59	7.27	8.72	4.63
By-product	5.45	0.90	3.64	1.95	0.42
AN (NA, 2-MN and DMN)	68.11	22.66	70.39	72.16	66.83
Conversion of 1-MN	73.56	23.56	74.03	74.11	67.25
Selectivity of AN	92.58	96.20	95.08	97.36	99.37

[a] Conditions: flow rate = 0.1 ml/min, pressure = 100 kPa, reaction temperature = 380 °C, time on stream = 2 h.

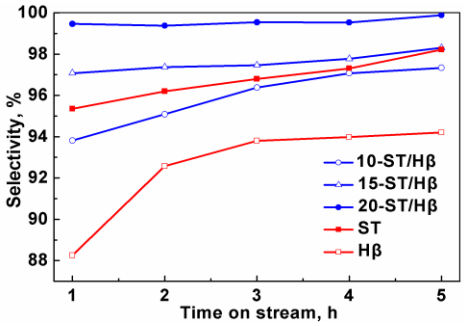

Fig. 8. The selectivity of AN over Hβ, ST, and X-ST/Hβ *vs.* TOS

The 1-MN conversion over ST and X-ST/Hβ is highly consistent with BET analysis, and can be ranked as follows: 10-ST/Hβ ≈ 15-ST/Hβ > 20-ST/Hβ >> ST. Fig. 9 shows the effects of time-on-stream (TOS) on catalytic performance of ST, Hβ, and X-ST/Hβ. The inferior stability of ST might be explained by its smaller number of weak and medium acid sites, low S_{BET}, and poor heat resistance [36]. 1-MN conversion on X-ST/Hβ shows similar stability to the parent Hβ. Therefore, a suitable synthesis method and ST loading content are advantageous to the surface acidity, textural properties, and catalytic activity of the catalysts X-ST/Hβ.

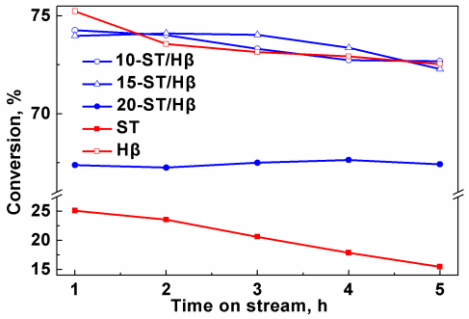

Fig. 9. The conversion of 1-MN over Hβ, ST, and X-ST/Hβ *vs.* TOS

3.3. Coke deposition

The carbonaceous deposition on spent catalysts was also measured by TG in O_2 atmosphere. As Fig. 10 depicts, the weight loss during the shift from 30 to 150 °C is ascribed to adsorbed gas and moisture. Subsequently, the weight of fresh catalyst stabilizes itself, whereas there is a 5 % weight loss for the used catalyst. We may attribute this to the formation of coke deposition, leading to the decrease of 1-MN conversion.

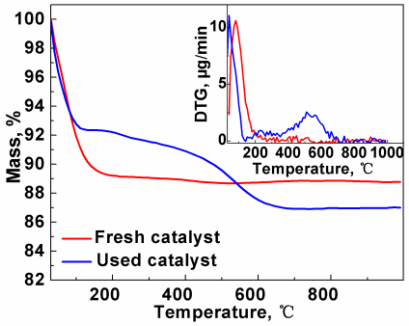

Fig. 10. TG and DTG (inset) profiles of fresh and used catalyst after 15 h of TOS

4. CONCLUSIONS

In this study, the catalysts X-ST/Hβ are synthesized, characterized, and tested for the conversion of 1-MN. After loading uniform ST on template containing zeolite Hβ, 10-15-ST/Hβ exhibited high S_{BET} and a substantial number of weak and moderately strong acidic sites. These sites were responsible for high 1-MN conversion. The microporous structure and fewer strong acid sites of 15-20-ST/Hβ were advantageous in the suppression of side reactions, accounting for its higher selectivity. Based on the current work's findings, catalyst 15-ST/Hβ improved alkyl naphthalene selectivity and yield.

Acknowledgments

This work was supported by the Key Discipline Construction of 211 Project IV in China [grant number 1843202543], the Research Innovation Program for College Graduates of Jiangsu Province [grant number KYLX15_0728], and the Science and Technology Program of Jiangsu Province [grant number BY2012003].

REFERENCES

1. **Lillwitz, L. D.** Production of Dimethyl-2,6-naphthalenedicarboxylate: Precursor to Polyethylene Naphthalene *Applied Catalysis A: General* 221 (1) 2001: pp. 337 – 358. https://doi.org/10.1016/S0926-860X(01)00809-2
2. **Jin, L.J., Zhou, X.J., Hu, H.Q., Ma, B.** Synthesis of 2,6-Dimethylnaphthalene by Methylation of 2-Methylnaphthalene on Mesoporous ZSM-5 by Desilication *Catalysis Communications* 10 (3) 2008: pp. 336 – 340.
3. **Nie, X.W., Janik, M.J., Guo, X.W., Song, C.S.** Shape-selective Methylation of 2-Methylnaphthalene with Methanol over H-ZSM-5 Zeolite: A Computational Study *The Journal of Physical Chemistry C* 116 (6) 2012: pp. 4071 – 4082. https://doi.org/10.1021/jp209337m
4. **Zhang, C., Guo, X.W., Song, C.S., Zhao, S.Q., Wang, X. S.** Effects of Steam and TEOS Modification on HZSM-5 Zeolite for 2,6-Dimethylnaphthalene Synthesis by Methylation of 2-Methylnaphthalene with Methanol *Catalysis Today* 149 (1 – 2) 2010: pp. 196 – 201.
5. **Chobsaard, A., Kraikul, N., Rangsunvigit, P., Kulprathipanja, S.** Influences of Solvents on the Production of High Purity 2,6-Dimethylnaphthalene via Catalytic Isomerization and Adsorptive Separation *Chemical Engineering Journal* 139 (1) 2008: pp. 78 – 83.
6. **Kraikul, N., Rangsunvigit, P., Kulprathipanja, S.** Integrations of Catalytic Isomerization to Adsorptive Separation for the Production of High Purity 2,6-Dimethylnaphthalene *Chemical Engineering Journal* 131 (1 – 3) 2007: pp. 145 – 153.
7. **Chawanwit, K., Bobuatong, K., Khongpracha, P., Tantirungrotechai, Y., Limtrakul, J.** Mechanistic Investigation on 1,5- to 2,6-Dimethylnaphthalene Isomerization Catalyzed by Acidic *β* Zeolite: ONIOM Study with an M06-L Functional *The Journal of Physical Chemistry C* 113 (36) 2009: pp. 16128 – 16137. https://doi.org/10.1021/jp904098t
8. **Popova, Z., Yankov, M., Dimitrov, L., Chervenkov, I.** Isomerization and Disproportionation of 1-MN on Zeolites *Reaction Kinetics and Catalysis Letters* 52 (1) 1994: pp. 51 – 58.
9. **Fedorynska, E., Winiarek, P.** Isomerization of Alkylaromatic Hydrocarbons on Nickel-boron-alumina Catalysts *Reaction Kinetics and Catalysis Letters* 54 (1) 1995: pp. 73 – 79. https://doi.org/10.1007/BF02071183
10. **Komatsu, T., Kim, J.H., Yashima, T.** MFI-type Metallosilicates as Useful Tools to Clarify What Determines the Shape Selectivity of ZSM-5 Zeolites *ACS Symposium Series* 738 (11) 1999: pp. 162 – 180.
11. **Takagi, Y., Nobusawa, T., Suzuki, T.** Prevention and Estimation of Catalytic Deactivation in Isomerization of 1-Methylnaphthalene *Kagaku Kogaku Ronbunshu* 21 (6) 1995: pp. 1096 – 1103. https://doi.org/10.1252/kakoronbunshu.21.1096
12. **Sun, H., Shi, S.J., Gu, Z.G.** Isomerization of Alkyl Naphthalene and Refining of 2-Methylnaphthalene *Chinese Journal of Chemical Engineering* 2016: 10.1016/j.cjche.2016.1008.1022.
13. **Li, T.L., Liu, X.Y., Wang, X.S.** Shape Selectivity for Disproportionation of Methylnaphthalene over Zeolite Hβ *Chinese Journal of Catalysis* 18 (3) 1997: pp. 221 – 224.
14. **Kang, N.Y., Chen, T., Lee, C.W., Choi, W.C., Lee, W.H., Park, S., Park, Y.K.** Catalytic Isomerization of Dimethyltetralin over Silicon- and Boron-Modified H-BEA Zeolites *Catalysis Letters* 132 (1 – 2) 2009: pp. 138 – 146.
15. **Jin, L.J., Fang, Y.M., Hu, H.Q.** Selective Synthesis of 2,6-Dimethylnaphthalene by Methylation of 2-Methylnaphthalene with Methanol on Zr/(Al)ZSM-5 *Catalysis Communications* 7 (5) 2006: pp. 255 – 259. https://doi.org/10.1016/j.catcom.2005.11.012
16. **Bai, X., Sun, K., Wu, W., Yan, P., Yang, J.** Methylation of Naphthalene to Prepare 2,6-Dimethylnaphthalene over Acid-dealuminated HZSM-12 Zeolites *Journal of Molecular Catalysis A: Chemical* 314 (1 – 2) 2009: pp. 81 – 87.
17. **Zhai, D.W., Yue, Y.H., Hua, W.M., Gao, Z.** Esterification and Transesterification on Al_2O_3-Doped Sulfated Tin Oxide Solid Acid Catalysts *Acta Physico-Chimica Sinica* 26 (7) 2010: pp. 1867 – 1872.
18. **Zhang, C., Liu, T., Wang, H.J., Wang, F., Pan, X.Y.** Synthesis of Acetyl Salicylic Acid over WO_3/ZrO_2 Solid Superacid Catalyst *Chemical Engineering Journal* 174 (1) 2011: pp. 236 – 241. https://doi.org/10.1016/j.cej.2011.09.010
19. **Krishnakumar, B., Velmurugan, R., Swaminathan, M.** TiO_2–SO_4^{2-} as a Novel Solid Acid Catalyst for Highly Efficient, Solvent Free and Easy Synthesis of Chalcones under Microwave Irradiation *Catalysis Communications* 12 (5) 2011: pp. 375 – 379. https://doi.org/10.1016/j.catcom.2010.10.015
20. **Reddy, B.M., Patil, M.K.** Organic Syntheses and Transformations Catalyzed by Sulfated Zirconia *Chemical Reviews* 109 (6) 2009: pp. 2185 – 2206.
21. **Arata, K.** Organic Syntheses Catalyzed by Superacidic Metal Oxides: Sulfated Zirconia and Related Compounds *Green Chemistry* 11 (11) 2009: pp. 1719 – 1728.
22. **Zhao, J., Yue, Y.H., Hua, W.M., He, H.Y., Gao, Z.** Catalytic Activities and Properties of Sulfated Zirconia Supported on Mesostructured γ-Al_2O_3 *Applied Catalysis A: General* 336 (1 – 2) 2008: pp. 133 – 139.
23. **Wang, Y.H., Gan, Y.T., Whiting, R., Lu, G.Z.** Synthesis of Sulfated Titania Supported on Mesoporous Silica Using Direct Impregnation and Its Application in Esterification of

Acetic Acid and n-Butanol *Journal of Solid State Chemistry* 182 (9) 2009: pp. 2530 – 2534. https://doi.org/10.1016/j.jssc.2009.07.003

24. **Shi, X.J., Wu, Y.L., Yi, H.F., Rui, G., Li, P.P., Yang, M.D., Wang, G.H.** Selective Preparation of Furfural from Xylose over Sulfonic Acid Functionalized Mesoporous SBA-15 Materials *Energies* 4 (12) 2011: pp. 669 – 684.
25. **Ye, F., Dong, Z.W., Zhang, H.J.** n-Hexane Isomerization over Copper Oxide-Promoted Sulfated Zirconia Supported on Mesoporous Silica *Catalysis Communications* 10 (15) 2009: pp. 2056 – 2059.
26. **Zhai, D.W., Nie, Y.Y., Yue, Y.H., He, H.Y., Hua, W.M., Gao, Z.** Esterification and Transesterification on Fe_2O_3-Doped Sulfated Tin Oxide Catalysts *Catalysis Communications* 12 (7) 2011: pp. 593 – 596. https://doi.org/10.1016/j.catcom.2010.12.020
27. **Prasetyoko, D., Ramli, Z., Endud, S., Nur, H.** TS-1 Loaded with Sulfated Zirconia as Bifunctional Oxidative and Acidic Catalyst for Transformation of 1-Octene to 1,2-Octanediol *Journal of Molecular Catalysis A: Chemical* 241 (1 – 2) 2005: pp. 118 – 125.
28. **Krishnan, C.K., Hayashi, T., Ogura, M.** A New Method for Post-Synthesis Coating of Zirconia on the Mesopore Walls of SBA-15 Without Pore Blocking *Advanced Materials* 20 (20) 2008: pp. 2131 – 2136. https://doi.org/10.1002/adma.200702822
29. **Laak, A.N.C.V., Zhang, L., Parvulescu, A.N., Bruijnincx, P.C.A., Weckhuysen, B.M., de Jong, K.P., de Jongh, P.E.** Alkaline Treatment of Template Containing Zeolites: Introducing Mesoporosity while Preserving Acidity *Catalysis Today* 168 (1) 2011: pp. 48 – 56. https://doi.org/10.1016/j.cattod.2010.10.101
30. **Zhao, H., Jiang, P.P., Dong, Y.M., Huang, M., Liu, B.L.** Effects of Morphology and Crystal Phase of Sulfated Nano-Titania Solid Acids on Catalytic Esterification *Reaction Kinetics Mechanisms and Catalysis* 113 (2) 2014: pp. 445 – 458.
31. **Noda, L.K., de Almeida, R.M., Probst, L.F.D., Gonçalves, N.S.** Characterization of Sulfated TiO_2 Prepared by the Sol-Gel Method and Its Catalytic Activity in the n-Hexane Isomerization Reaction *Journal of Molecular Catalysis A: Chemical* 225 (1) 2005: pp. 39 – 46. https://doi.org/10.1016/j.molcata.2004.08.025
32. **Smirniotis, P.G., Ruckenstein, E.** Platinum Impregnated Zeolite β as a Reforming Catalyst *Catalysis Letters* 17 (3) 1993: pp. 341 – 347.
33. **Flanigen, E.M., Khatami, H., Szymanski, H.A.** Infrared Structural Studies of Zeolite Frameworks *Advances in Chemistry* 101 (16) 1974: pp. 201 – 229.
34. **Zhu, M.L., Li, S., Li, Z.X., Lu, X.M., Zhang, S.J.** Investigation of Solid Catalysts for Glycolysis of Polyethylene Terephthalate *Chemical Engineering Journal* 185 – 186 (8) 2012: pp. 168 – 177.
35. **Hwang, C.C., Mou, C.Y.** Comparison of the Promotion Effects on Sulfated Mesoporous Zirconia Catalysts Achieved by Alumina and Gallium *Applied Catalysis A: General* 365 (2) 2009: pp. 173 – 179. https://doi.org/10.1016/j.apcata.2009.06.007
36. **Shi, X.J., Wu, Y.L., Li, P.P., Yi, H.F., Yang, M.D., Wang, G.H.** Catalytic Conversion of Xylose to Furfural over the Solid Acid $SO_4^{2-}/ZrO_2–Al_2O_3$/SBA-15 Catalysts *Carbohydrate Research* 346 (4) 2011: pp. 480 – 487. https://doi.org/10.1016/j.carres.2011.01.001